

1. Supporting Text

POF Synthesis: Benzene-1,4-dicarboxaldehyde (BDA, 134 mg, 1.0 mmol) was added into 100 mL propionic acid and the solution was stirred for 10 mins. Then, the solution was supplemented 1.0 mL trifluoroacetic acid (TFA) and 5.0 mL nitrobenzene (NBZ) as the catalyst and the oxidant, respectively. After that, pyrrole (0.14 mL, 2.0 mmol) was added dropwise into the above solution under stirring. The mixture was kept at 130°C for 12.0 h under successively stirring and cooled to room temperature to render a dark suspension. The product was filtered and washed with ethanol, chloroform, and ethanol to remove unreacted reagents and small porphyrin molecules. POF was finally obtained as black powders after dried at 60°C for 24 h.

Synthesis of G@POF: G@POF was synthesized through otherwise identical methods as POF with graphene (G) added as the template. G was obtained by thermally reducing graphene oxide at high temperature. Typically, 700 mg G was added into the propionic acid solution of BDA, TFA, and NBZ under the same condition as the above POF synthesis. The theoretical mass ratio of G:POF is determined to be 3:1. The slurry was then sonicated for 30 min for intensive mixing of G and the reactants. After pyrrole was added, the mixture was maintained at 130°C for 12.0 h under continuous stirring. G@POF was obtained after purification using the same methods as POF.

Synthesis of G@POF-Fe: G@POF-Fe was synthesized and purified using similar procedures as G@POF with Fe²⁺ introduced as central ion coordinated within porphyrin rings. Iron acetate (Fe(CH₃COO)₂, 620 mg, 2.5 mmol) was added after pyrrole and the mixture was stirred for another 10 min for intensive solvation. The molar ratio of Fe²⁺

to porphyrin unit is 5:1 to guarantee the coordination.

Fabrication of G@POF-Fe modified Separators: 1.0 mg of poly(vinylidene fluoride) (PVDF) binder and 9.0 mg G@POF-Fe power were scattered in N-methyl-2-pyrrolidone (NMP) by strong ultrasonication for 2.0 h. Then, 40.0 mL of the dispersion was filtered on four piece of a PP membrane (commercial Celgard 2400) and subsequently dried at 60°C for 24.0 h. The areal loading of G@POF-Fe on the PP membrane was 0.14 mg cm⁻².

Fabrication of Sulfur Cathodes: Slurry coating method was used to prepare the sulfur cathode. The slurry was prepared by mixing commercial sulfur powders (purity: 99.99%), carbon nanotubes, and PVDF as the binder with desirable ratio in NMP, then the evenly mixed slurry was coated onto aluminum foils using a doctor-blade method, dried in the oven at 60°C for 24 h, then punched into disks.

Structural Characterization: The morphology of the modified separator was characterized by a JSM 7401F (JEOL Ltd., Tokyo, Japan) SEM operated at 3.0 kV and a JEM 2010 (JEOL Ltd., Tokyo, Japan) TEM operated at 120.0 kV. Energy-dispersive X-ray spectrometer (EDS) measurements were performed on the JEM 2010 TEM equipped with an Oxford Instrument energy dispersive X-ray spectrometer. XPS characterization was analyzed on a SI5 Thermo VG ESCALAB250 surface analysis system with Al-K_α radiation. The membrane conductivity of the composite separator was obtained using conventional the KDY-1 four-probe method. Fourier transform infrared spectrometry (FTIR) was performed on a NEXUS 870 spectrograph.

Electrochemical Evaluation: The standard 2025 coin-type cells were assembled

in an Ar-filled glove box, employing sulfur cathode, lithium foil as anode, and different separators for battery performance evaluation. The electrolyte was 1.0 M lithium bis(trifluoromethanesulfonyl)imide that dissolved in the solution of 1,3-dioxolane (DOL) and 1,2-dimethoxyethane (DME) (v/v = 1:1) with 2 wt% of lithium nitrate (LiNO_3). 25 μL electrolyte was added to the cell with sulfur loading of 1.33 mg cm^{-2} and 40 μL for 6.54 mg cm^{-2} sulfur loading. The galvanostatic mode of the tested coin-type cells was 1.7–2.8 V using a Land multichannel battery cycler. The electrochemical impedance spectroscopy (EIS) measurements and CV were performed on a Solartron 1470E electrochemical workstation.

2. Supporting Figures

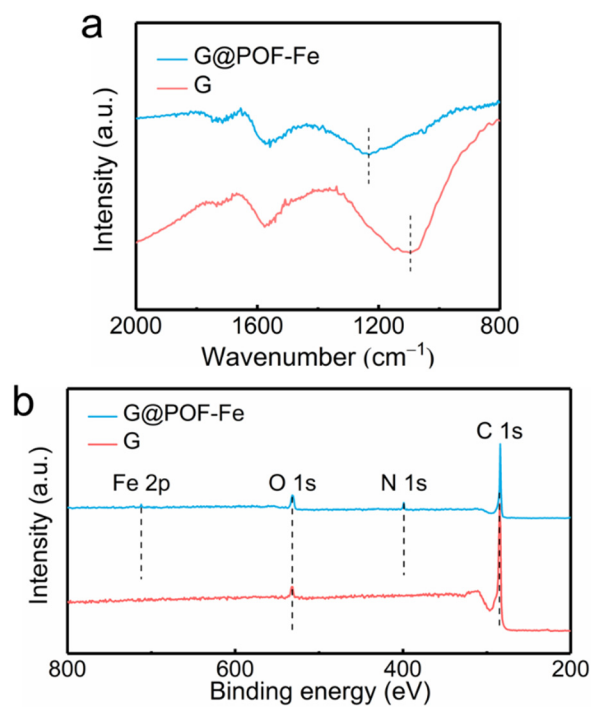


Figure S1. (a) FTIR spectra and (b) XPS survey spectra G@POF-Fe and G.

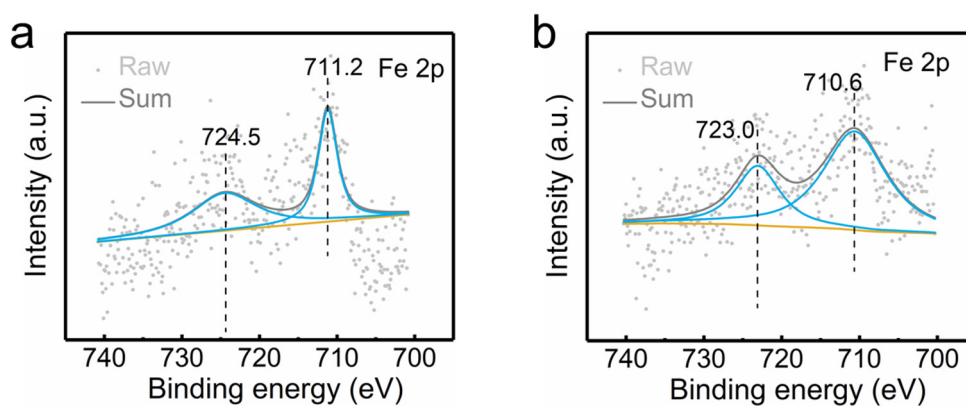


Figure S2. XPS Fe 2p spectrum of (a) G@POF-Fe and (b) G@POF-Fe-Li₂S₆.

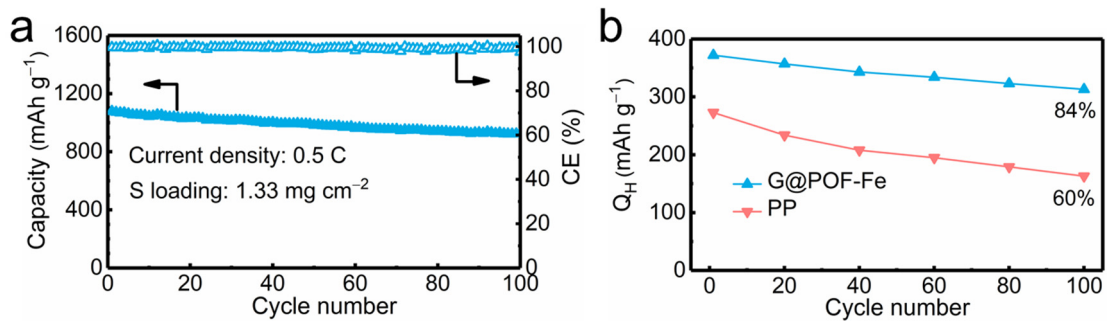


Figure S3. (a) The cycling performance of G@POF-Fe cells at 0.5 C for 100 cycles and (b) the corresponding discharge capacity retention of the upper plateaus.

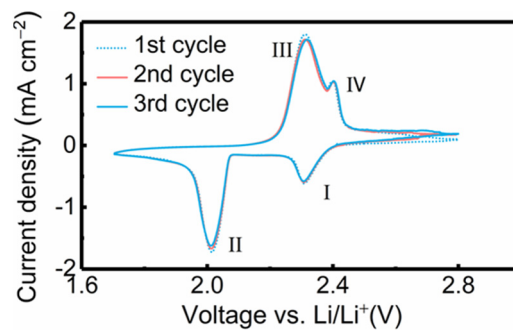


Figure S4. CV analysis for the G@POF-Fe cell.

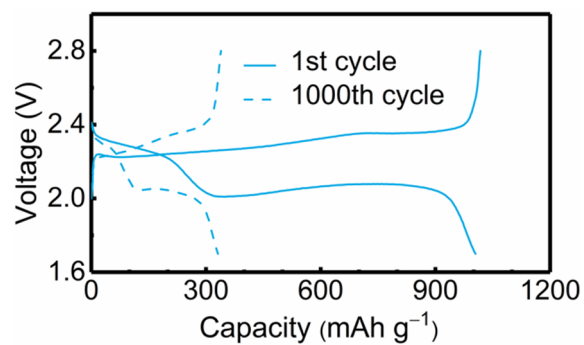


Figure S5. Discharge/charge curves of G@POF-Fe cells at 1 C.

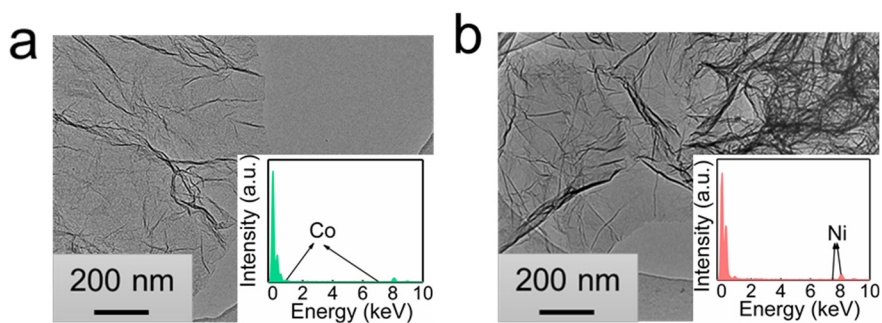


Figure S6. TEM images of (a) G@POF-Ni and (b) G@POF-Co. The inset figures are corresponding EDS analysis results.

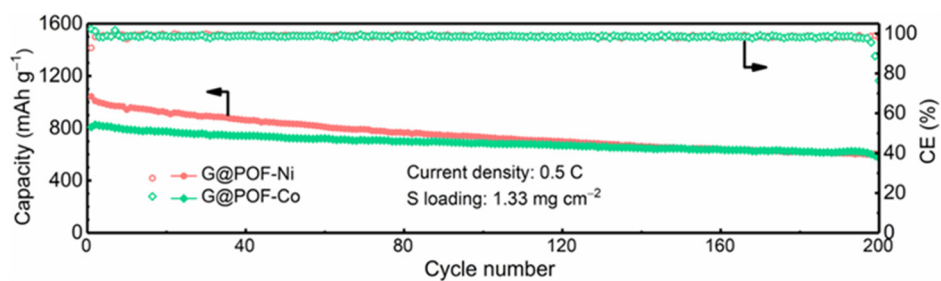


Figure S7. Cycling performance of cells with different interlayers at 0.5 C.

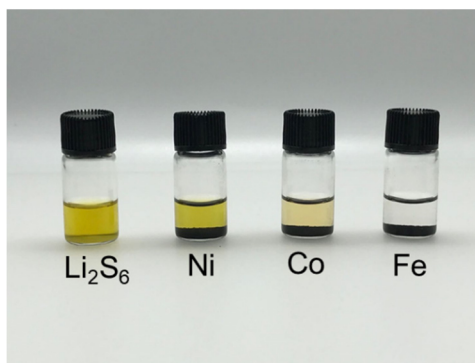


Figure S8. Static adsorption of Li_2S_6 solutions by various adsorbents after 3.0 h.